Cellular/Molecular

Neuronal Phenotype Dependency of Agonist-Induced Internalization of the 5-HT_{1A} Serotonin Receptor

Elodie Bouaziz,[1,2,3] Michel Boris Emerit,[1,2,3] Guilan Vodjdani,[3,4] Vanessa Gautheron,[3,4] Michel Hamon,[1,2,3] Michèle Darmon,[1,2,3] and Justine Masson[1,2,3]

[1]Centre de Psychiatrie et Neurosciences, INSERM UMR 894, Paris F-75014, France, [2]Université Paris Descartes, Sorbonne Paris Cité, Paris 75270, France, [3]Université Pierre et Marie Curie, Paris F-75013, France, and [4] Centre de Recherche de l'Institut du Cerveau et de la Moelle Epinière, CNRS UMR-7225, INSERM UMR-975, Paris F-75013, France

Selective serotonin reuptake inhibitors (SSRI) are aimed at increasing brain 5-HT tone; however, this expected effect has a slow onset after starting SSRI treatment because of initial activation of 5-HT_{1A} autoreceptor-mediated negative feedback of 5-HT release. After chronic SSRI treatment, 5-HT_{1A} autoreceptors desensitize, which allows 5-HT tone elevation. Because 5-HT_{1A} receptor (5-HT_{1A}R) internalization has been proposed as a possible mechanism underlying 5-HT_{1A} autoreceptor desensitization, we examined whether this receptor could internalize under well controlled *in vitro* conditions in the LLC-CPK1 cell line and in raphe or hippocampal neurons from rat embryos. To this goal, cells were transfected with recombinant lentiviral vectors encoding N-terminal tagged 5-HT_{1A}R, and exposed to various pharmacological conditions. Constitutive endocytosis and plasma membrane recycling of tagged-5-HT_{1A}R was observed in LLC-PK1 cells as well as in neurons. Acute exposure (for 1 h) to the full 5-HT_{1A}R agonists, 5-HT and 5-carboxamido-tryptamine, but not the partial agonist 8-OH-DPAT, triggered internalization of tagged 5-HT_{1A}R in serotonergic neurons only. In contrast, sustained exposure (for 24 h) to all agonists induced tagged-5-HT_{1A}R endocytosis in raphe serotonergic neurons and a portion of hippocampal neurons, but not LLC-PK1 cells and partial agonist displayed an effect only in serotonergic neurons. In all cases, agonist-induced tagged 5-HT_{1A}R endocytosis was prevented by the 5-HT_{1A}R antagonist, WAY-100635, which was inactive on its own. These data showed that agonist-induced 5-HT_{1A}R internalization does exist in neurons and depends on agonist efficacy and neuronal phenotype. Its differential occurrence in serotonergic neurons supports the idea that 5-HT_{1A}R internalization might underlie 5-HT_{1A} autoreceptor desensitization under SSRI antidepressant therapy.

Key words: **5-HT_{1A} receptor; constitutive and drug-induced internalization; hippocampus; neuron; raphe; recycling**

Introduction

Serotonin (5-hydroxytryptamine, 5-HT) is involved in the control of mood, emotion, and in various psychiatric diseases. Notably depression and generalized anxiety are causally linked, at least in part, to a dysfunction of the serotonergic system (Stahl et al., 2013). To date, the most widely used antidepressants are selective inhibitors of serotonin reuptake (SSRI) leading to the idea that their therapeutic efficacy is mediated by an increase in extracellular 5-HT and the stimulation of serotonergic receptors. Among the numerous 5-HT receptors, the 5-HT_{1A} type (5-HT_{1A}R) has been proposed to play a key role in the mechanisms of antidepressant/anxiolytic actions of SSRI (Lanfumey and Hamon, 2000; Blier and Ward, 2003; Hensler, 2003). 5-HT_{1A}R is confined to the somatodendritic compartment of both serotonergic neurons and target neurons of serotonergic projections where it acts as autoreceptor and heretoreceptor, respectively. The long-term tonic stimulation of 5-HT_{1A}R by 5-HT that occurs during chronic SSRI treatment has been shown to affect differentially 5-HT_{1A} autoreceptors in the dorsal raphe nucleus (DRN) and 5-HT_{1A} heteroreceptors in the hippocampus. Both *in vivo* and *in vitro* electrophysiological studies showed that a 2–3 week treatment with SSRI results in a functional desensitization of 5-HT_{1A} autoreceptors, without affecting postsynaptic 5-HT_{1A}R in hippocampus. Accordingly, after chronic SSRI treatment, the potency of direct 5-HT_{1A}R agonists to hyperpolarize the plasma membrane is markedly reduced in DRN serotonergic neurons, but is unaffected in hippocampal CA1 neurons (Lanfumey and Hamon, 2000). Although numerous *in vivo* studies have been performed to elucidate what the cellular processes that underlie such brain region specificity of 5-HT_{1A}R desensitization are, the question is still largely unsolved. SSRI-induced desensitization of 5-HT_{1A} autoreceptors has been proposed to involve changes at the transcription level; however, these changes could not be correlated to modifications at the protein level (Le Poul et al., 2000).

Received Jan. 10, 2013; revised Oct. 30, 2013; accepted Nov. 18, 2013.

Author contributions: E.B., M.D., and J.M. designed research; E.B., M.B.E., G.V., V.G., and J.M. performed research; G.V. contributed unpublished reagents/analytic tools; E.B., M.H., M.D., and J.M. analyzed data; E.B., M.H., M.D., and J.M. wrote the paper.

This research has been supported by grants from INSERM, University Pierre et Marie Curie, and the FPEC program ("Newmood"; LSHM-CT-2803-503474). J.M. and G.V. are supported by Centre National de la Recherche Scientifique. E.B. received fellowships from FRM and NerF during performance of this work. Confocal imaging was performed at the Imagerie Cellulaire facilities at the Pitié-Salpêtrière and PICPEN of CPN. We are grateful to Morgane Moulin for highly reliable technical help.

Correspondence should be addressed to Justine Masson, INSERM U894, 2ter rue d'Alésia, 75014 Paris, France. E-mail: justine.masson@inserm.fr.

DOI:10.1523/JNEUROSCI.0186-13.2014

 0270-6474/14/340282-13$15.00/0

Studies from Riad et al. (2001, 2004) using immunocytochemical labeling coupled to electron microscopy, provided evidence that SSRI treatment induced 5-HT$_{1A}$R internalization in neurons in the raphe but not in the hippocampus. However, only acute treatment but not chronic treatment with SSRIs apparently produced a decreased expression of 5-HT$_{1A}$R at the somatodendritic plasma membrane of DRN neurons (Riad et al., 2008), in sharp contradiction with the idea that receptor internalization could mediate, at least in part, chronic SSRI-induced functional desensitization demonstrated by electrophysiological recordings.

Because *in vivo* approaches have obvious limitations to investigate agonist-regulated receptor traffic in specific neuronal phenotypes, we addressed the question of 5-HT$_{1A}$R internalization and its control using the LLC-PK1 cell line and primary cultures of serotonergic raphe versus hippocampal neurons. Immunostaining strategies and live imaging allowed thorough studies of the traffic of 5-HT$_{1A}$R between plasma membrane and intracellular compartments under basal conditions and after acute or sustained exposure to 5-HT$_{1A}$R ligands. Striking differences between DRN serotonergic neurons and other cell types clearly showed that 5-HT$_{1A}$R agonist-induced internalization depends on agonist efficacy and cell phenotype.

Materials and Methods

Experiments were performed in strict agreement with the institutional guidelines for use of animals and their care, in compliance with national and international laws and policies 24 (Council directives no. 87–848, October 19, 1987, Ministère de l'Agriculture et de la Forêt, Service Vétérinaire de la Santé et de la Protection Animale, permission no. 75–805 to J.M.).

Gestating female Sprague Dawley rats (Charles River Breeding Center) were maintained under controlled environmental conditions (21 ± 1°C, 60% relative humidity, 12 h light/dark cycle), with food and water available *ad libitum* until killed for embryo removal.

Antibodies and markers. The following primary antibodies were used: anti-Flag M2 monoclonal antibody (1:2000; Sigma), rabbit anti-5-HT polyclonal antibody (1:100,000; Calbiochem). The secondary antibodies used were anti-mouse and anti-rabbit IgG Alexa Fluor 488- and 594-conjugated antibodies (1:500; Invitrogen), anti-mouse chicken IgG Alexa Fluor 594-conjugated antibody (1:800; Invitrogen), and anti-chicken goat IgG Alexa Fluor 488-conjugated antibodies (1:500; Invitrogen). LysoTracker Red DND-99 (100 nM), Transferrin-Alexa Fluor 546 conjugate (1:1000 or 5 μg/ml), α-bungarotoxin-Alexa Fluor 488 and 555 (BTX-AF488 and BTX-AF555, 1:1000) were purchased from Invitrogen. [^{125}I]Tyr^{54}-α-bungarotoxin ([^{125}I]BTX) was purchased from PerkinElmer.

Chemicals and drugs. Monensin sodium (used at 80 μM), sucrose (0.35 M), (±)-8-Hydroxy-2 (dipropylamino)-tetralin hydrobromide (8-OH-DPAT; 1–10 μM), 5-carboxamido-tryptamine maleate (5-CT; 1 μM), 5-HT (10 μM), WAY-100635 maleate (1–10 μM), methiothepin (1–10 μM), and spiperone (10 μM) were purchased from Sigma. D-Tubocurarine (10 μM) was purchased from Serlabo and [^{3}H] lysergic acid diethylamide ([^{3}H]LSD; 79.2 Ci/mmol) and [^{35}S]GTPγS (1000 Ci/mmol) were purchased from GE Healthcare.

Plasmids. The rat 5-HT$_{1A}$R encoding sequence (Albert et al., 1990) was first inserted between the HindIII and EcoRI sites of the pCB6 vector, then a double-strand oligonucleotide coding sequence (5′AGCTATGT CAGGGCTCCAGGGAGCTCTCGTAGTATCTCCACAT-3′) for the minimum site of recognition for α-bungarotoxin (BTX), BTX binding site (BBS) (Sekine-Aizawa and Huganir, 2004) was inserted in the HindIII sites to generate the BBS-5-HT$_{1A}$ construct. Plasmids encoding the rab4-GFP and rab5-GFP were as described previously (Sönnichsen et al., 2000).

Cell cultures and transfection. LLC-PK1 cells were grown in DMEM (Invitrogen) supplemented with 4.5 g/L glucose, GlutaMAX I (Invitrogen), 10% fetal bovine serum, 10 U/ml penicillin G, and 10 mg/ml streptomycin. For stable transfection, the cDNA encoding BBS-5-HT$_{1A}$ was transfected in LLC-PK1 cells by electroporation using the Gene Pulser Xcell electroporation system (Bio-Rad; 135 V, 1800 μF in 200 μl of DMEM containing 5–10 × 10^{6} cells and 5–10 μg plasmid DNA; relaxation time: ~40 ms). Clones expressing the neomycin resistance marker were selected in G418 (1.25 mg/ml)-containing medium (Langlois et al., 1996). After two passages, G418-resistant colonies were screened by observation of BTX fluorescence, and stably transfected clones were maintained in 0.4 mg/ml G418. For transient transfection, the cDNAs encoding rab4-GFP or rab5-GFP were transfected in BBS-5-HT$_{1A}$ stably transfected LLC-PK1 cells with Lipofectamine 2000 (Invitrogen). Cells were used 24 h after transfection.

[^{125}I]BTX binding assay. Wild-type or transfected LLC-PK1 cells were washed once with DMEM-free serum and incubated with [^{125}I]BTX (1 nM) for 20 min at 20°C. Nonspecific binding was measured by adding cold BTX (100 nM) during [^{125}I]BTX incubation. After one DMEM wash, cells were lysed with 0.1 M NaOH for 15 min to extract [^{125}I]BTX bound and cell lysate radioactivity was quantified using a Beckman gamma counter.

Preparation of membranes. Wild-type or transfected LLC-PK1 cells were washed with Dulbecco's phosphate buffer saline (DPBS; Invitrogen), scraped into Tris buffer (50 mM Tris-HCl, pH 7.4), and homogenized with a Polytron. After each of four successive washings in Tris buffer, the membranes were collected by centrifugation at 31,000 × *g* for 20 min at 4°C. An incubation for 10 min at 37°C was performed after the first washing to eliminate 5-HT (from the serum in the culture medium), and the final pellet was suspended in the same Tris buffer to be stored at −80°C until use. Protein concentration was measured using BCA protein assay kit (Pierce).

Radioligand binding assays. Binding assays were performed using 1.6 nM [^{3}H]LSD and 4–20 μg of membrane proteins in 500 μl of 50 mM Tris-HCl, pH 7.4, supplemented with or without "cold" ligands at various concentrations. Samples were incubated for 90 min at 25°C, until rapid filtration through Whatman GF/B filters that had been precoated with polyethylenimine (0.5% v/v). Subsequent filter washing, counting of entrapped radioactivity, and calculations of relevant binding parameters were as described previously (Carrel et al., 2006). For the determination of B_{max} and K_d values (INPLOT ver. 4 program), binding assays were performed with various concentrations of [^{3}H]LSD ranging between 1 and 60 nM. Triplicate determinations were made for each assay conditions.

[^{35}S]GTP-γ-S binding assays. [^{35}S]GTPγS binding onto membranes from stably transfected LLC-PK1 cells was measured according to a procedure adapted from Carrel et al. (2006). Briefly, membranes (~50 μg protein) were incubated for 30 min at 37°C in a final volume of 800 μl assay buffer (50 mM Tris-HCl, pH 7.4, 4 mM $MgCl_2$, 160 mM NaCl, 0.25 mM EGTA) containing 0.1 nM [^{35}S]GTPγS, 300 μM GDP with or without 5-HT$_{1A}$R ligands (1 μM), or BTX (100 μM). The reaction was terminated by addition of 3 ml ice-cold 50 mM Tris-HCl buffer and rapid vacuum filtration through Whatman GF/B filters. Each filter was then placed into 4.5 ml scintillation fluid and its entrapped radioactivity measured using a Beckman counter. Basal [^{35}S]GTPγS binding was determined from samples without 5-HT$_{1A}$R ligands or BTX. Triplicate determinations were made for each assay conditions.

Lentiviral vector construction and production. BBS sequence was inserted upstream of the Flag-5-HT$_{1A}$R sequence (Carrel et al., 2006) in the expression plasmid pTrip-PGK-ΔU3 (SmaI/XhoI). Stocks of viral particles were produced as described previously (Zennou et al., 2000; Poulain et al., 2008). HEK293T cells were transiently cotransfected with the pTrip-BBS-Flag-5-HT$_{1A}$R plasmid vector, the p8.9 encapsidation plasmid, and the pHCMV-G (vesicular stomatitis virus pseudotype) envelope plasmid by calcium phosphate precipitation. Briefly, the supernatants were collected 48 h after transfection, treated with DNase I (Roche Diagnostics) before ultracentrifugation, and then resuspended in PBS, aliquoted, and finally stored at −80°C until use. p24 capsid protein was quantified with an HIV-1 p24 ELISA antigen assay (Beckman Coulter). Lentiviral stocks averaged 50 ng/μl p24 antigen.

Neuronal cell culture and lentiviral-mediated transduction. Neuronal cultures from hippocampi were made as described previously (Carrel et al., 2006) with slight modifications. Briefly, hippocampi were dissected from rat embryos at E18, incubated with trypsin, and tissue dissociation was achieved with a Pasteur pipette. Cells were counted and plated on

poly-D-lysine-coated 14 mm diameter coverslips in a 10 cm dish, at a density of 1000,000–1200,000 cells per dish (128–154 cells/mm^2), in complete Neurobasal medium supplemented with B27 (Invitrogen), GlutaMAX I 100×, 10 U/ml penicillin G, and 10 mg/ml streptomycin. For raphe neuron cultures, the brainstem area with B4–B9 raphe nuclei was dissected from rat embryos at E14, and tissue dissociation and plating were done as for hippocampal neurons except that raphe neurons were plated at a density of 2200,000–2500,000 cells per dish (280–320 cells/mm^2). Two hours after plating, the culture medium was replaced by conditioned medium obtained by incubating glial cell cultures (70–80% confluency) for 24 h in the complete medium described above. Conditioned medium was used as such or supplemented with the recombinant lentiviral vector suspension encoding BBS-Flag-5-HT$_{1A}$R. Neurons were kept with the same medium up to 12–14 days *in vitro* (DIV) for allowing receptor expression high enough for subsequent assays.

Immunofluorescence. Cells on coverslips were washed with DPBS+ (DPBS containing 0.1 mM $CaCl_2$ and 0.1 mM $MgCl_2$) at 37°C, then fixed with 3% paraformaldehyde containing 4% sucrose (PFA/sucrose) at 37°C in DPBS+ and permeabilized with 0.1% Triton X-100 in DPBS (without $CaCl_2$, $MgCl_2$). After two washes (10 min) in DPBS, cells were incubated for 30 min in antibody buffer (3% bovine serum albumin, 2% normal goat serum, 2% normal donkey serum in DPBS). Incubation with primary antibodies was then performed in antibody buffer at room temperature (1 h). After two washes in DPBS, incubation with secondary antibodies proceeded for 1 h. The secondary antibodies used were Alexa Fluor-conjugated goat anti-rabbit IgG or anti-mouse IgG. The coverslips were finally mounted in Fluoromount-G solution (CliniSciences) for immunofluorescence visualization using confocal microscopy.

Internalization experiments and immunocytofluorescent labeling of internalized receptors. For all experiments, cells were washed once with serum-free medium and incubations with pharmacological compounds were performed in serum-free medium. For [^{125}I]BTX internalization experiments, cells were first incubated with [^{125}I]BTX for 20 min at 12°C, washed with DMEM, and then exposed to drugs at 20°C. Cells were then subjected to a 15 min acid wash (150 mM NaCl, 50 mM acetic acid) to release [^{125}I]BTX bound to plasma membranes. Finally, cells were lysed with 0.1 NaOH to extract [^{125}I]BTX bound to internalized receptors. [^{125}I]BTX contained in acid wash and cell lysate was quantified using a Beckman gamma counter.

For fluorescence experiments with cell lines, LLC-PK1 cells were incubated with BTX-AF488 (1:1000) for 30 min at 4°C, washed with DMEM and incubated at 37°C for 30 min, or incubated with BTX-AF488 (1:1000) plus drugs, or none, directly at 37°C for 15, 30, or 60 min. Transferrin Alexa Fluor 546 conjugate or LysoTracker Red DND-99 was added to the medium with BTX conjugate during the whole internalization experiment or the last 30 min of incubation, respectively. Membrane-bound BTX conjugate was removed with a 15 min acid wash and cells were fixed with PFA/sucrose. For experiments with infected neurons, primary mouse anti-Flag antibody (1:2000) was complexed with secondary anti-mouse chicken Alexa Fluor 594 antibody (1:800; fluorescent antibody complex) in Neurobasal medium/HEPES 20 mM during 45 min at room temperature before incubation with neurons. Acute treatment consisted of exposing neurons (12–14 DIV) to ligands (10 μM) for 1 h at 37°C, whereas a pretreatment with ligands (10 μM) for 24 h before the 1 h exposure to the antibody complex was performed for sustained treatment. Cells were fixed and incubated with anti-chicken goat Alexa Fluor 488 antibody (1:500) without permeabilization to label receptors that were still present on plasma membranes. For neurons from raphe cultures, cells were then permeabilized to detect 5-HT with anti-5-HT antibodies.

Microscopy. Immunofluorescence images were generated using a Leica TCS SP2 AOBS laser scanning confocal microscope (63× oil-immersion lens). Contrast and brightness were chosen to ensure that all pixels were within the linear range. Images were the product of threefold line averages. In all cases, emission and excitation filters proper to each fluorophore were used sequentially and the absence of cross talk between different channels was checked with selectively labeled preparations. Leica pictures (.lei) were saved as TIFF images and plates were assembled using Adobe Photoshop CS2 (Adobe Systems). Background was lowered using Gaussian blur (radius 1 pixel) and contrast and brightness of images displayed in figures were modified using Adobe Photoshop CS2 only for illustrations.

Image analysis. For receptor distribution assays in LLC-PK1 cells, quantification of the internalized receptors was done on cells that had been exposed to a 15 min acid wash to remove cell membrane receptor's labeling. Fluorescence was measured using ImageJ on 30 cells per condition. For analysis of colocalization of BTX with rab4-GFP and rab5-GFP, images were median filtered (1 pixel), threshold was adjusted, and colocalization was quantified by colocalization threshold. For receptor distribution assay in neurons, images of individual cells were obtained with a 2.2× zoom. Total and intracellular fluorescence were quantified on a region of interest (ROI) for 19–84 neurons per condition. Cells were randomly chosen with phenotypic consideration to avoid dead, dividing, or receptor overexpressing cells. Total levels of receptor expression were quantified as fluorescence obtained for each cell with the secondary anti-mouse chicken Alexa Fluor 594 antibody labeling. Intracellular labeling was quantified as the Alexa Fluor 594 antibody labeling inside an ROI delimited into the neuron just inside the cell membrane. Internalized receptors were quantified as the ratio of intracellular labeling to total labeling.

Live cell imaging. Experiments were performed on stably transfected LLC-PK1 cells or transduced raphe neurons grown on 35 mm glass base dishes (IWAKI) with culture medium supplemented with 20 mM HEPES. Time-lapse imaging was performed at 37°C using a spinning-disk microscope mounted on an inverted motorized confocal microscope (Leica TCS SP2) through a 100×1.4 NA PL-APO objective lens. The apparatus is composed of a Yokogawa CSU-22 spinning disk head, a Roper Scientific laser lounge, a Photometrics Coolsnap HQ2 CCD camera for image acquisition, and MetaMorph software (MDS) to control the setup. Acquisition parameters were 100–300 ms exposure for the GFP channel. Laser was set to 30% in each case. Movies shown in figures correspond to stacks resulting from a maximal intensity projection through the *z*-axis performed with the MetaMorph software (National Institutes of Health Image). Trajectories of moving vesicles were tracked with the MTrackJ Plugin of ImageJ software developed by Erik Meijering (Biomedical Imaging Group Rotterdam of the Erasmus MC–University Medical Center Rotterdam, The Netherlands).

Statistical analyses. Data are presented as means ± SEM. Statistical significance was assessed using one-way or two-way ANOVA followed by Dunnett's or Bonferroni's test. Critical level of significance was set at $p \leq 0.05$.

Results

BBS and Flag tagged 5-HT$_{1A}$ receptors are properly targeted and functional

We developed two constructs of the 5-HT$_{1A}$R, one tagged with a sequence coding for BBS for cell line transfection (BBS-5-HT$_{1A}$; Fig. 1*A1*), and the other tagged with BBS and a Flag sequence for primary cultured rat E14 raphe and E18 hippocampal neuron lentiviral vector transduction (BBS-Flag-5-HT$_{1A}$, Fig. 1*A2*). These tags were added at the N-terminal tail of the receptor to allow visualization of 5-HT$_{1A}$R that was trafficking from its functional localization, the plasma membrane, using fluorophore-conjugated BTX or anti-Flag antibodies (Fig. 1*B*). BBS fusion proteins were previously shown to be appropriate to follow AMPA receptor trafficking (Sekine-Aizawa and Huganir, 2004), GABA$_B$ receptor (Hannan et al., 2011), and 5-HT$_3$ receptor internalization (Morton et al., 2011). In permeabilized cells expressing tagged-5-HT$_{1A}$R, a strong perinuclear BTX labeling was observed, presumably corresponding to BBS-5-HT$_{1A}$R newly synthetized and still localized in endoplasmic reticulum or Golgi apparatus in both transfected LLC-PK1 cells (Fig. 1*B1*, arrowhead) and transduced hippocampal neurons (Fig. 1*B3*, arrowhead). Surface labeling with fluorescent BTX or Flag immunofluorescent staining performed on fixed cells without permeabiliza-

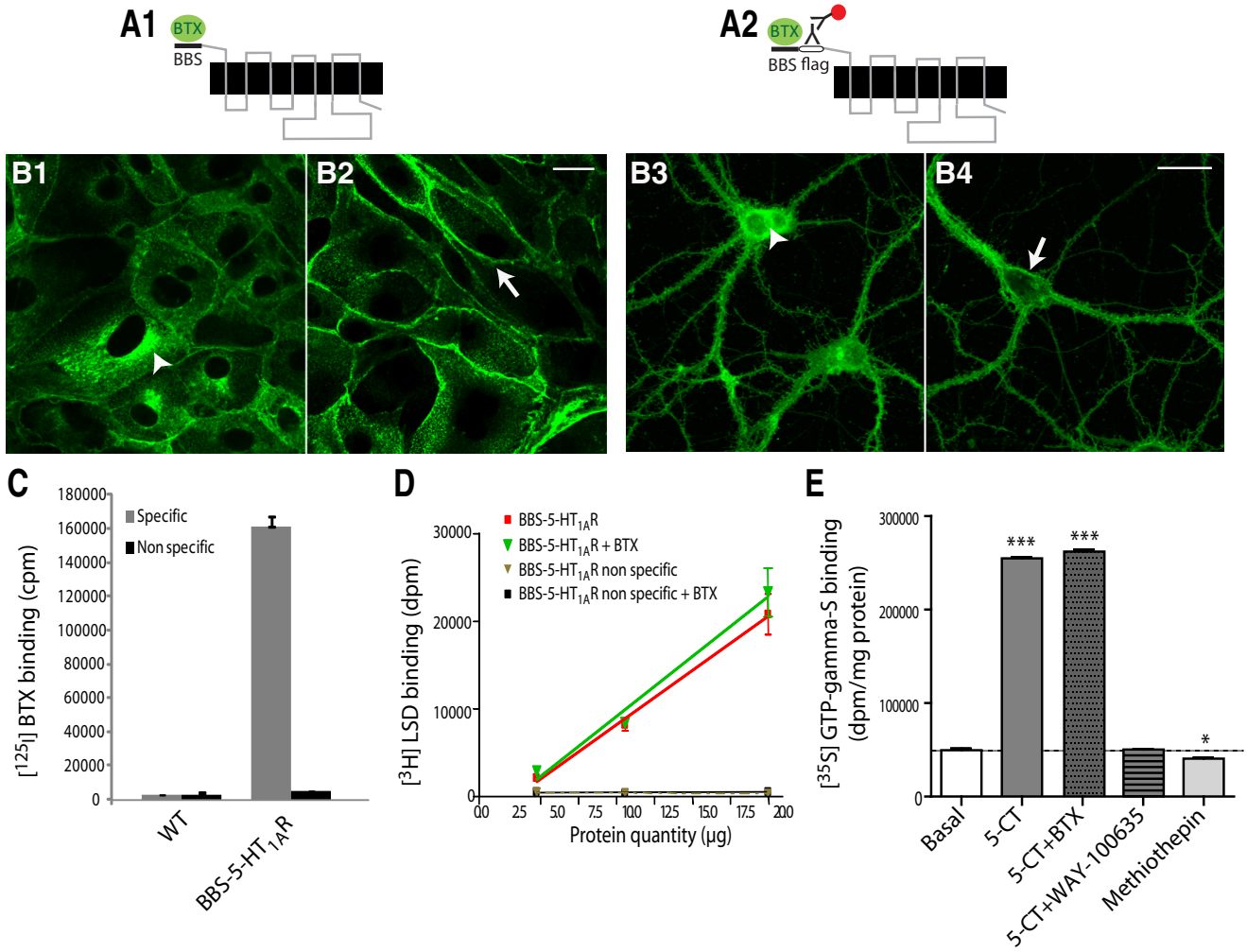

Figure 1. BBS-5-HT$_{1A}$R and BBS-Flag-5-HT$_{1A}$R constructs: expression, pharmacology, and coupling. ***A***, Schematic illustration of the folding of the membrane-integrated BBS-5-HT$_{1A}$R and BBS-Flag-5-HT$_{1A}$. The minimum site for BTX recognition site, BBS, is alone (***A1***) or combined with a Flag tag (***A2***) genetically fused to the N-terminus domain of 5-HT$_{1A}$R. BBS binds BTX and tag Flag is recognized by an anti-Flag antibody that can be labeled by a fluorescent secondary antibody (antibody complex). ***B***, Confocal microscopy images of BBS-5-HT$_{1A}$R and BBS-Flag-5-HT$_{1A}$ stained by (1) BTX-AF488 in permeabilized (***B1***, arrowhead; endoplasmic reticulum labeling) or intact-transfected (***B2***, arrow; plasma membrane labeling) LLC-PK1 cells or (2) antibody complex in transduced permeabilized (***B3***, arrowhead; endoplasmic reticulum labeling) or intact (***B4***, arrow; plasma membrane labeling) neurons in primary culture from E18 hippocampus. Scale bars: 20 μm. ***C***, Specific [^{125}I]BTX binding to LLC-PK1 cells transfected or not (WT) with BBS-5-HT$_{1A}$R. Nonspecific binding was quantified with [^{125}I]BTX (1 nM) plus unlabeled BTX (100 nM). ***D***, [^{3}H]LSD binding without or with BTX (100 μM) onto membranes from BBS-5-HT$_{1A}$R-transfected LLC-PK1 cells. Nonspecific binding was determined with [^{3}H]LSD plus 10 μM 5-HT. ***E***, Effects of 5-CT (1 μM), alone or with BTX (100 μM) or WAY-100635 (1 μM), and methiothepin (1 μM) on [^{35}S]GTPγS binding to membranes from BBS-5-HT$_{1A}$R-transfected LLC-PK1 cells. One-way ANOVA, Dunnett's test, $^{*}p < 0.05$, $^{***}p < 0.001$.

tion demonstrated a strong basolateral plasma membrane localization of the BBS-5-HT$_{1A}$R in LLC-PK1 cells (Fig. 1*B2*, arrow) and of BBS-Flag-5-HT$_{1A}$R in the soma and dendrites of hippocampal neurons (Fig. 1*B4*, arrow). In these two models, targeting of BBS-5-HT$_{1A}$R and BBS-Flag-5-HT$_{1A}$R was similar to that of tagged 5-HT$_{1A}$R used in previous studies (Langlois et al., 1996; Jolimay et al., 2000).

To verify the specificity of BTX binding onto BBS-5-HT$_{1A}$R, [^{125}I]BTX binding assays were performed with nontransfected (WT) or stably expressing BBS-5-HT$_{1A}$R LLC-PK1 cells. No specific [^{125}I]BTX binding was observed onto WT cells, whereas stably expressing BBS-5-HT$_{1A}$R LLC-PK1 cells were endowed with a high specific [^{125}I]BTX binding capacity (Fig. 1*C*). Using [^{3}H]LSD as radioligand to label 5-HT$_{1A}$R (Darmon et al., 1998), we also observed that BTX (100 nM) did not interfere with its specific binding to BBS-5-HT$_{1A}$R (Fig. 1*D*). Determination of the affinity constant of [^{3}H]LSD binding onto BBS-5-HT$_{1A}$R gave a K_d value of 10.6 nM, closely similar to that previously obtained with untagged 5-HT$_{1A}$R (Darmon et al., 1998). Further characterization of BBS-5-HT$_{1A}$R showed a 5-fold increase in γ-[^{35}S]-GTP binding after 5-CT (1 μM) stimulation confirming a coupling to $G_{i/o}$ protein. As illustrated in Figure 1*E*, the 5-CT effect was prevented by the 5-HT$_{1A}$R antagonist WAY-100635 (1 μM), as previously shown with native 5-HT$_{1A}$R (Carrel et al., 2006). Moreover, the 5-HT$_{1A}$R inverse agonist methiothepin (1 μM; Martel et al., 2007) significantly reduced basal γ-[^{35}S]-GTP binding by 18.1% suggesting that BBS-5-HT$_{1A}$R was constitutively activated (Fig. 1*E*). Finally, 5-CT-stimulated γ-[^{35}S]-GTP binding onto membranes from LLC-PK1 cells did not differ whether or not cells had been incubated with BTX (Fig. 1*E*). These results indicated that BBS incorporation into the N terminus of the 5-HT$_{1A}$R did not alter its pharmacological profile and functional responses to ligands (Langlois et al., 1996; Darmon et al., 1998). Overall, the inserted BBS had the capacity to operate as a functionally silent reporter of 5-HT$_{1A}$R trafficking.

Tagged-5-HT$_{1A}$ receptors are constitutively internalized in transfected LLC-PK1 cells and in transduced neurons

Extracellular BBS and Flag tag allow overcoming limitations observed with GFP fusion proteins to study receptor endocytosis. Indeed, such GFP fusion proteins can perturb localization and signaling of the tagged receptor and its interactions with partner proteins, mainly because of steric constraints due to the relatively large size of GFP (238 amino acids). Furthermore, with such fusion proteins, it is impossible to distinguish internalized receptors from receptors on the way to the plasma membrane. Usually, cycloheximide is used to limit *de novo* receptor synthesis, but this drug inhibits all protein synthesis, which could alter trafficking mechanisms that need biosynthesis of regulatory proteins. In contrast, BBS tag allowed the labeling of the receptor at the plasma membrane and its follow up during its intracellular traffic.

In LLC-PK1 cells stably expressing BBS-5-HT$_{1A}$R, fluorescent BTX bound onto BBS-5-HT$_{1A}$R at 4°C was localized exclusively at the plasma membrane (Fig. 2*A1*). When cells were placed at 37°C for 30 min in serum-free medium, the BBS-5-HT$_{1A}$R labeled by fluorescent BTX was observed within intracellular structures with vesicular appearance (Fig. 2*A2*). To clearly identify intracellular BBS-5-HT$_{1A}$R from BBS-5-HT$_{1A}$R that was still localized at the plasma membrane, we performed a labeling protocol with an acid wash. In a first step, BBS-5-HT$_{1A}$R-expressing cells were exposed to fluorescent BTX-AF488 (green) in serum-free medium at 37°C for 1 h (Fig. 2*B1*). Then, half of living LLC-PK1 cells expressing BBS-5-HT$_{1A}$R were acid washed (Fig. 2*B2*) to unlabel the plasma membrane while the other half was maintained under control conditions (Fig. 2*B1*). After fixation, BBS-5-HT$_{1A}$R still bound to the plasma membrane could be labeled using BTX-AF555 (red). This strategy allowed labeling of internalized receptor (green) or plasma membrane-bound receptor (Fig. 2*B1*, yellow or *B2*, red). In complementary experiments, we used the same acid wash strategy after labeling BBS-5-HT$_{1A}$R with [^{125}I]BTX. We determined that after 20 min at 20°C, BBS-5-HT$_{1A}$R internalization followed by intracellular [^{125}I]BTX accumulation reached 11.42 ± 0.84% of total [^{125}I]BTX binding in control conditions and neither 5-HT (10 μM), the 5-HT$_{1A}$R partial agonist 8-OH-DPAT (10 μM), alone or in combination with the antagonist WAY100635 (10 μM), nor 5-HT$_{1A}$R inverse agonists (methiothepin and spiperone, 10 μM), added during incubation with [^{125}I]BTX significantly affected BBS-5-HT$_{1A}$R internalization (Fig. 2*C*).

We then investigated the intracellular pathway followed by constitutively internalized BBS-5-HT$_{1A}$R. In LLC-PK1-transfected cells, constitutive BBS-5-HT$_{1A}$R endocytosis was found to follow the same pathway as transferrin (TRF) endocytosis (Fig. 3*A1*). In particular, both BBS-5-HT$_{1A}$R and TRF internalizations were blocked by high sucrose (0.35 M), an inhibitor of clathrin-coated pits-mediated endocytosis (Fig. 3*A2*,*B*). In addition, monensin, a cation ionophore that blocks recycling (Stein et al., 1984), produced a significant increase in intracellular BBS-5-HT$_{1A}$R, indicating that BBS-5-HT$_{1A}$R normally underwent recycling to the plasma membrane (Fig. 3*A3*,*B*). Further experiments were performed using cells transfected with rab5-GFP or rab4-GFP, markers of early endosomes and fast recycling vesicles (Rosenfeld et al., 2002; Seachrist and Ferguson, 2003). After 15 min of internalization, 67% of vesicles labeled with BBS-5-HT$_{1A}$R were expressing rab5-GFP (Fig. 3*C1*) and 72% of vesicles labeled with BBS-5-HT$_{1A}$R were expressing rab4-GFP when internalization was pursued to 30 min (Fig. 3*C2*). Live confocal imaging on LLC-PK1 BBS-5-HT$_{1A}$R-expressing cells clearly identified BBS-5-HT$_{1A}$R endocytosis and recycling events (Fig. 3*D*, arrow). The weak colabeling of internalized BBS-5-HT$_{1A}$R with LysoTracker Red-DND99, a marker of late endosomes, showed that BBS-5-HT$_{1A}$R was scarcely degraded 1 h after internalization (Fig. 3*E*). Altogether, these results suggested that the constitutively internalized BBS-5-HT$_{1A}$R in LLC-PK1 cells followed a clathrin-coated pitted endocytic pathway, and were mainly sorted to a fast recycling pathway with low degradation.

For experiments on neurons, acid wash strategy could not be used to determine whether constitutive internalization occurred as in LLC-PK1 cells because it was too damaging for cells. After incubation, in a serum-free medium, at 37°C for 60 min with a fluorescent antibody complex, vesicular structures endowed with BBS-Flag-5-HT$_{1A}$R (Fig. 4*A*, arrows) could be detected in the soma of hippocampal (Fig. 4*A3*) and serotonergic raphe (Fig. 4*B3*; identified by 5-HT immunostaining) neurons. Internalized BBS-Flag-5-HT$_{1A}$R (Fig. 4*A2*,*B2*, red) could be clearly differentiated from BBS-Flag-5-HT$_{1A}$R still localized at the cell membrane (Fig. 4*A1*,*B1*, green; *A3*,*B3*, yellow). Quantification showed that 9% of BBS-Flag-5-HT$_{1A}$R were internalized in soma and proximal dendrites of serotonergic raphe neurons, under basal conditions, in the absence of receptor ligands (Fig. 4*C*). A pretreatment (24 h) with WAY-100635 (10 μM) or spiperone (10 μM) had no effect on BBS-Flag-5-HT$_{1A}$R endocytosis in serotonergic raphe neurons, suggesting that BBS-Flag-5-HT$_{1A}$R internalization was not induced by endogenous 5-HT released in raphe culture and was independent of any constitutive activity of the receptor. In living neurons also, we showed that the tagged-5-HT$_{1A}$R underwent internalization followed by a rapid recycling that could be visualized on the time lapse of live confocal imaging showing single events of internalization and recycling (Fig. 4*D*, arrows). Internalized tagged-5-HT$_{1A}$R were trafficking inside the soma or anterogradely between the soma and proximal dendrites (Fig. 4*E*, arrows).

Agonist-dependent endocytosis of BBS-Flag-5-HT$_{1A}$R depends on the neuronal phenotype, agonist strength, and duration of stimulation

Under our primary culture conditions, raphe cultures at 14 DIV contained equal amounts of glial cells and neurons, and among them, ~10% were serotonergic. Among the latter neurons, the proportion of those expressing BBS-Flag-5-HT$_{1A}$R ranged between 45 and 75% from one experiment to another. In all cases, analyses were performed on neurons with comparable levels of BBS-Flag-5-HT$_{1A}$R expression. Interestingly, levels of BBS-Flag-5-HT$_{1A}$R were not modified by sustained agonist treatments (Table 1), indicating that quantification of BBS-Flag-5-HT$_{1A}$R internalization quantification could not be biased by changes in expression receptor levels, thereby discarding the possible occurrence of nonspecific activation of the promotor controlling receptor expression, as can be observed in transfected cell lines (Cowen et al., 1997).

No change in BBS-Flag-5-HT$_{1A}$R endocytosis was observed in serotonergic raphe neurons after cell incubation for 1 h with the partial 5-HT$_{1A}$R agonist, 8-OH-DPAT (10 μM; Assié et al., 1999; Fig. 5*A*,*B*). However, a marked increase of internalized BBS-Flag-5-HT$_{1A}$R fraction, up to 260% of control, was observed in serotonergic raphe neurons after an incubation with 8-OH-DPAT for 24 h (Fig. 5*A*,*B*). This effect was specific of the serotonergic neuron phenotype because no internalization was detected in nonserotonergic neurons either after acute or sustained treatment with 8-OH-DPAT (Fig. 5*B*, right graph). On the

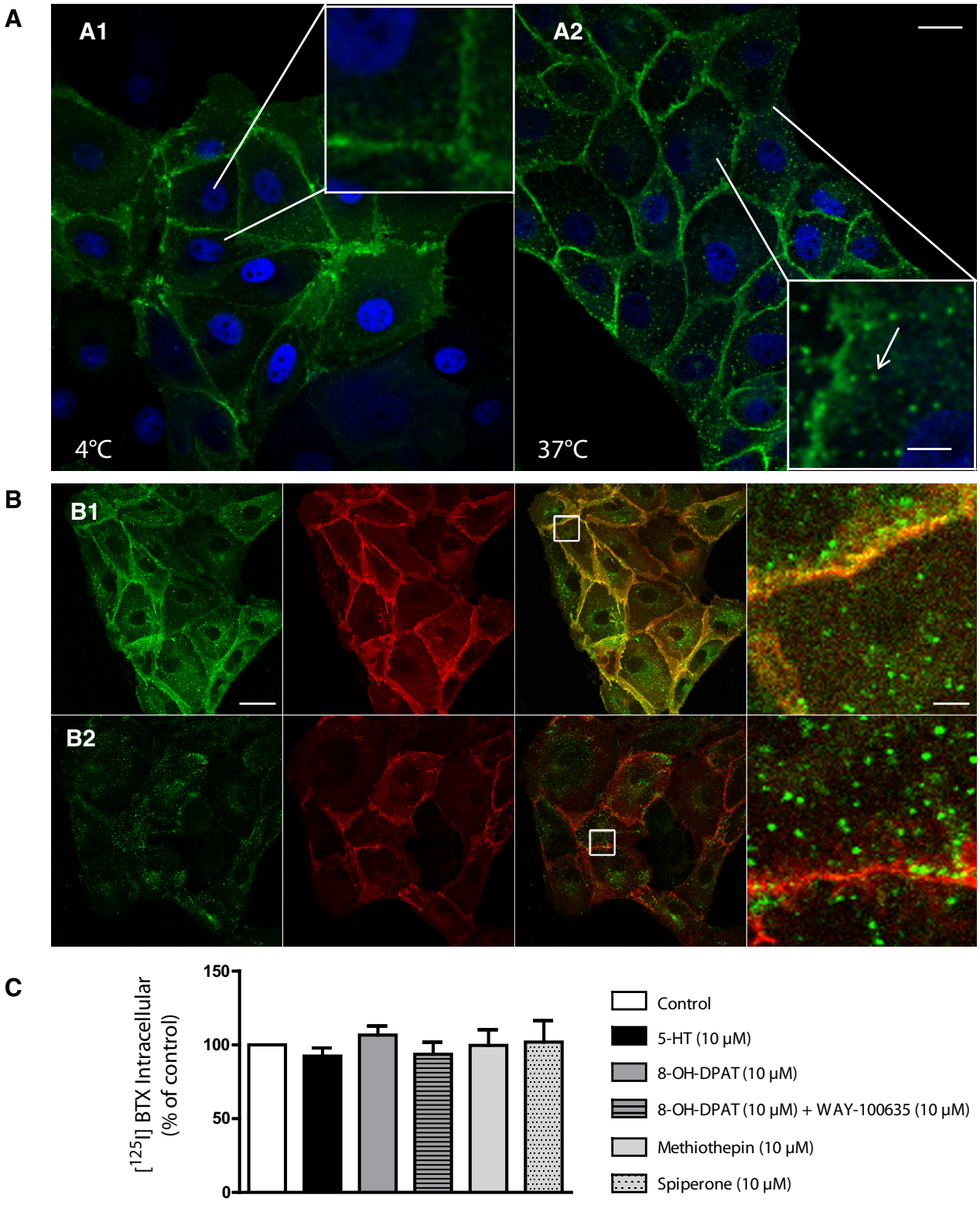

Figure 2. Tagged-5-HT$_{1A}$R internalization in stably transfected LLC-PK1 cells. ***A***, BTX-AF488 binds to cells at 4°C (***A1***; 30 min) in serum-free medium, then cells are immediately fixed or incubated 30 min at 37°C (***A2***). At 4°C, binding of fluorescent BTX-AF488 is restricted to the plasma membrane (***A1***), whereas an intracellular (vesicular) fluorescence is observed after BBS-5-HT$_{1A}$R internalization at 37°C (***A2***, arrow). ***B***, BTX-AF488 binds to cells and internalizes during 1 h at 37°C (green labeling). After washing, cells are directly fixed (***B1***) or fixative conditions are preceded by a 15 min acid wash to remove bound BTX-AF488 from plasma membrane (***B2***). After fixation, all cells are incubated for 10 min with BTX-AF555 to label plasma membrane-bound BBS-5-HT$_{1A}$R (red labeling). Right, Enlargements of white squares in merge pictures to illustrate the efficiency of acid wash to remove plasma membrane-bound BTX (no yellow labeling in ***B2*** compared with ***B1***). ***C***, 5-HT$_{1A}$R internalization quantified by intracellular [^{125}I]BTX binding in transfected LLC-PK1 cells incubated for 20 min with various 5-HT$_{1A}$R ligands (5-HT, 8-OH-DPAT alone or with WAY100635, and inverse agonists methiothepin or spiperone; all ligands at 10 μM). Entrapped (intracellular) [^{125}I]BTX radioactivity measured after acid wash is expressed as a percentage of total [^{125}I]BTX binding. Scale bars: ***A***, 20 and 4 μm in enlarged boxes; ***B***, 20 and 2 μm in zoom (right).

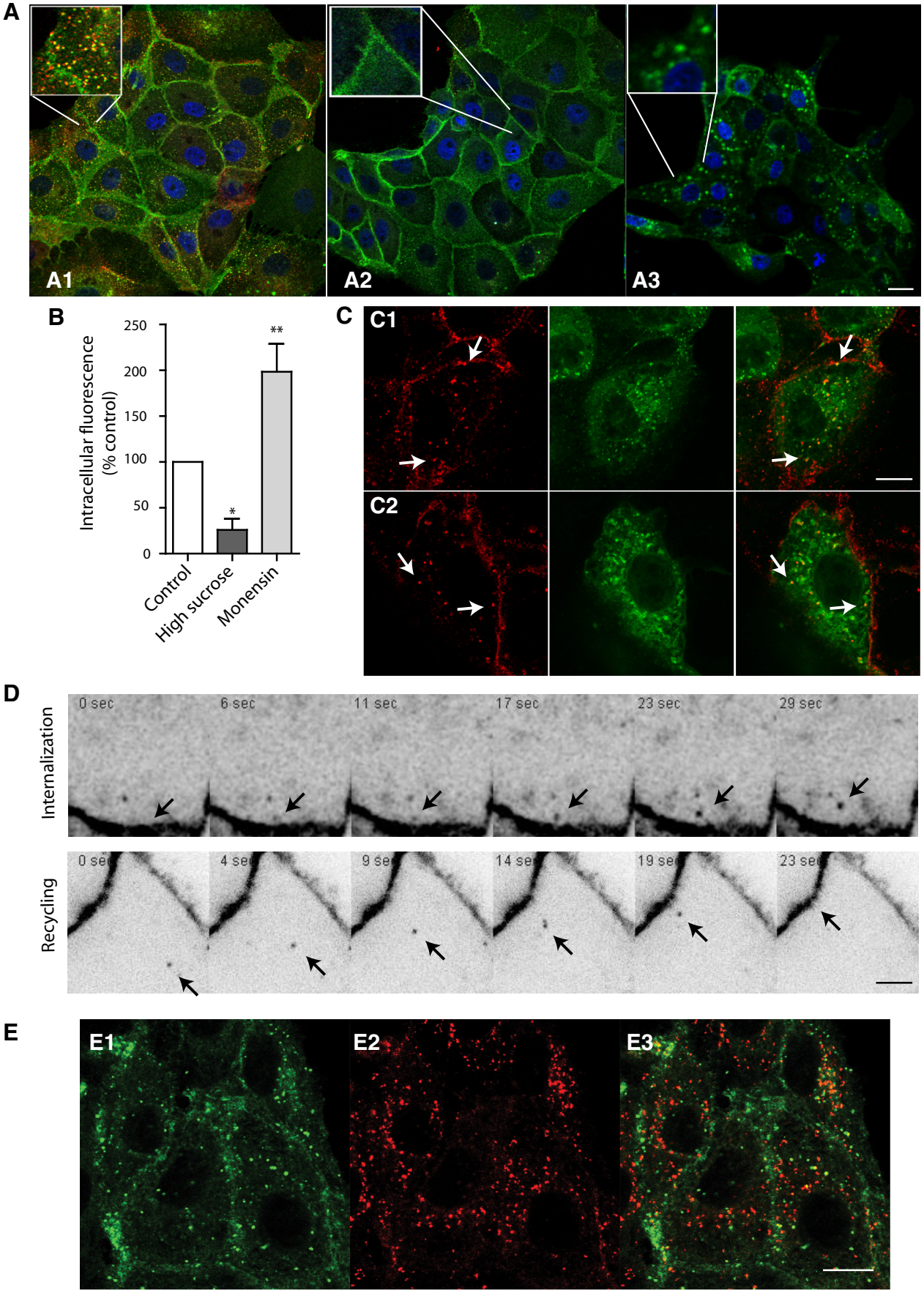
A
A1
A2
A3
B
Intracellular fluorescence (% control)
250
200
150
100
50
0
**
*
Control
High sucrose
Monensin
C
C1
C2
D
Internalization
0 sec
6 sec
11 sec
17 sec
23 sec
29 sec
Recycling
0 sec
4 sec
9 sec
14 sec
19 sec
23 sec
E
E1
E2
E3

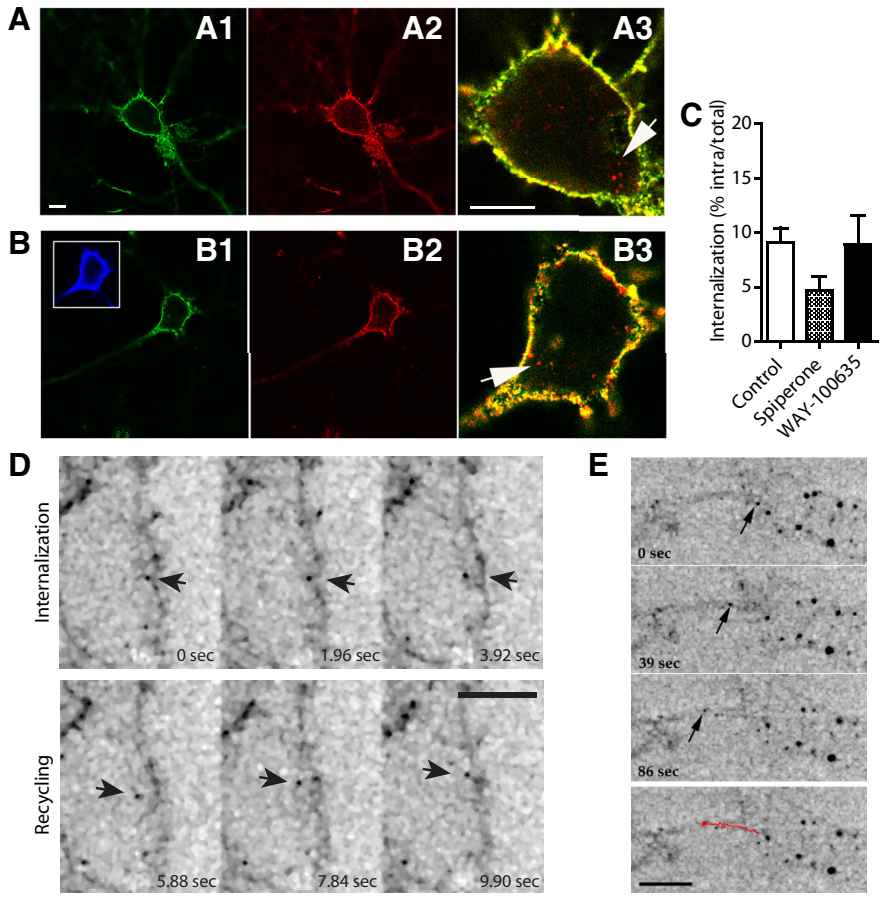

Figure 4. Traffic of BBS-Flag-5-HT$_{1A}$R in a transduced neuron. ***A***, ***B***, Immunostaining of hippocampal (***A***) and serotonergic raphe (***B***) neurons expressing BBS-Flag-5-HT$_{1A}$R. BBS-Flag-5-HT$_{1A}$Rs localized at the plasma membrane were labeled in green (***A1***, ***B1***), total BBS-Flag-5-HT$_{1A}$R in red (***A2***, ***B2***), and internalized BBS-Flag-5-HT$_{1A}$Rs were identified on merge picture (***A3***, ***B3***) by red labeling (arrows) compared with yellow plasma membrane BBS-Flag-5-HT$_{1A}$R. Serotonergic raphe neurons were labeled with anti 5-HT antibodies after permeabilization (***B1***, blue). ***C***, Quantification of internalized BBS-Flag-5-HT$_{1A}$R in serotonergic raphe neurons in control conditions and after exposure to spiperone or WAY-100635. ***D***, ***E***, Inverted monochrome images from time-lapse imaging of hippocampal neurons expressing BBS-Flag-5-HT$_{1A}$R. ***D***, Single events of internalization from plasma membrane and recycling in BBS-Flag-5-HT$_{1A}$R-transduced neuron during a time lapse of 9.90 s (arrow). ***E***, Intracellular anterograde traffic of BBS-Flag-5-HT$_{1A}$R along proximal dendrites. Red line represents the traveled distance of BBS-Flag-5-HT$_{1A}$R-positive vesicle (arrow) in 86 s. Scale bars: 5 μm.

other hand, the two full 5-HT$_{1A}$R agonists, 5-CT and 5-HT (Assié et al., 1999), induced BBS-Flag-5-HT$_{1A}$R endocytosis after 1 h treatment only, up to the same level as that noted after a 24 h treatment with 8-OH-DPAT. As shown in Figure 5,*A* and *B*, in all cases, agonist-induced BBS-Flag-5-HT$_{1A}$R internalization in serotonergic raphe neurons was prevented when WAY-100635 (10 μM) was added with the agonist. Increases in total receptor endocytosis after 24 h treatment (Fig. 5*B*) were the consequence of a shift of the maximum frequency of neurons displaying higher internalization levels with agonists (14% for 8-OH-DPAT, 16% for 5-HT, and 22% for 5-CT) compared with control (4%; Fig. 5*C*). Altogether, these data showed that 5-CT was the more potent agonist to induce receptor internalization.

In contrast, whether treatment with 8-OH-DPAT was acute or sustained, this partial 5-HT$_{1A}$R agonist did not induce BBS-Flag-5-HT$_{1A}$R internalization in hippocampal neurons (Fig. 6*A–C*). Similarly, 1 h treatment with the two full agonists, 5-CT and 5-HT, had no effect on receptor endocytosis (Fig. 6*A*,*B*, left graph). However, when hippocampal neurons were exposed for 24 h to either of the latter two agonists, they exhibited a heterogeneous response, with no internalization in some (LOW) neurons but a high level of internalization (HIGH) in others. Quantitative analyses showed that LOW neurons, with an internalization rate (0–10%) at the same low level as under basal (without drug) conditions, represented 59.6 and 65.1% of all hippocampal neurons exposed to 5-CT and 5-HT, respectively (Fig. 6*C*, LOW). The other 40.4 and 34.9% of neurons, respectively, corresponded to those that presented a clear-cut full agonist-induced BBS-Flag-5-HT$_{1A}$R internalization, with an internalization rate up to 30% (Fig. 6*C*, HIGH).

Therefore, BBS-Flag-5-HT$_{1A}$R was faintly but constitutively internalized in both raphe and hippocampal neurons. However, agonist-induced BBS-Flag-5-HT$_{1A}$R internalization depended on neuronal population, efficacy of (partial or full) agonists, and duration of treatment with these ligands.

←

Figure 3. Constitutive internalization and recycling in stably transfected LLC-PK1 cells expressing BBS-5-HT$_{1A}$R. ***A***, Cells are incubated 30 min at 37°C with BTX-AF488 and transferrin-A546 (TRF; 10 μg/ml; ***A1***, ***A2***), and in the presence of 0.35 M sucrose (***A2***) to block clathrin-mediated endocytosis or with 80 μM monensin (***A3***) to block recycling, respectively. Merge pictures point out the colocalization of BTX (in green) in control condition (***A1***), whereas both BTX and TRF endocytosis were blocked by high sucrose treatment (***A2***). ***B***, Internalized BBS-5-HT$_{1A}$R is measured in control conditions and during inhibition of internalization (high sucrose) or recycling (monensin). Data are presented as mean ± SEM integrated fluorescence corresponding to intracellular BTX-AF488 in four independent experiments (300 cells). ***C***, Colocalization of internalized BTX-labeled-BBS-5-HT$_{1A}$R with rab5-GFP (***C1***) and rab4-GFP (***C2***) after 15 and 30 min of BTX-AF555 incubation at 37°C, respectively. In merged pictures (right), yellow labeling shows BTX and rab-GFP colocalization (arrows). ***D***, Individual internalization or recycling events (arrows) were identified using live confocal microscopy and shown as time lapse. ***E***, Localization of entrapped BTX-AF488 in lysosomes. BBS-5-HT$_{1A}$R internalized (***E1***) do not colocalize with lysosome-labeled with LysoTracker (***E2***) on merged picture (***E3***). *$p < 0.05$, **$p < 0.001$ as compared with control (one-way ANOVA, Dunnett's test). Scale bars: ***A***, 20 μm; ***C***, ***E***, 10 μm; ***D***, 2 μm.

Discussion

We investigated the trafficking properties of the 5-HT$_{1A}$R expressed in the LLC-PK1 cell line and raphe versus hippocampal neurons in primary culture. For this purpose, we developed a new functional construct, BBS-tagged-5-HT$_{1A}$R, which allowed visualization of 5-HT$_{1A}$R endocytosis and recycling. Our data showed that the receptor underwent a constitutive, agonist-independent internalization in both LLC-PK1 cells and rat brain neurons. The internalized receptor followed the clathrin-dependent pathway and was predominantly recycled back to the plasma membrane, with very little degradation. In addition, agonist-dependent 5-HT$_{1A}$R internalization was demonstrated in neurons, with striking differences between serotonergic raphe neurons and nonserotonergic neurons in raphe and hippocampus.

Table 1. Level of BBS-Flag-5-HT$_{1A}$ receptor expression in transduced serotonergic raphe neurons in control condition and after sustained pharmacological treatment with 5-HT$_{1A}$R agonists

	Control ($n = 51$)	8-OH-DPAT 24 h ($n = 36$)	5-CT 24 h ($n = 19$)	5-HT 24 h ($n = 19$)
Level of BBS-Flag-5-HT$_{1A}$R expression (% control)	0.999 ± 0.6161	1.011 ± 0.1091	1.231 ± 0.2300	1.084 ± 0.0964

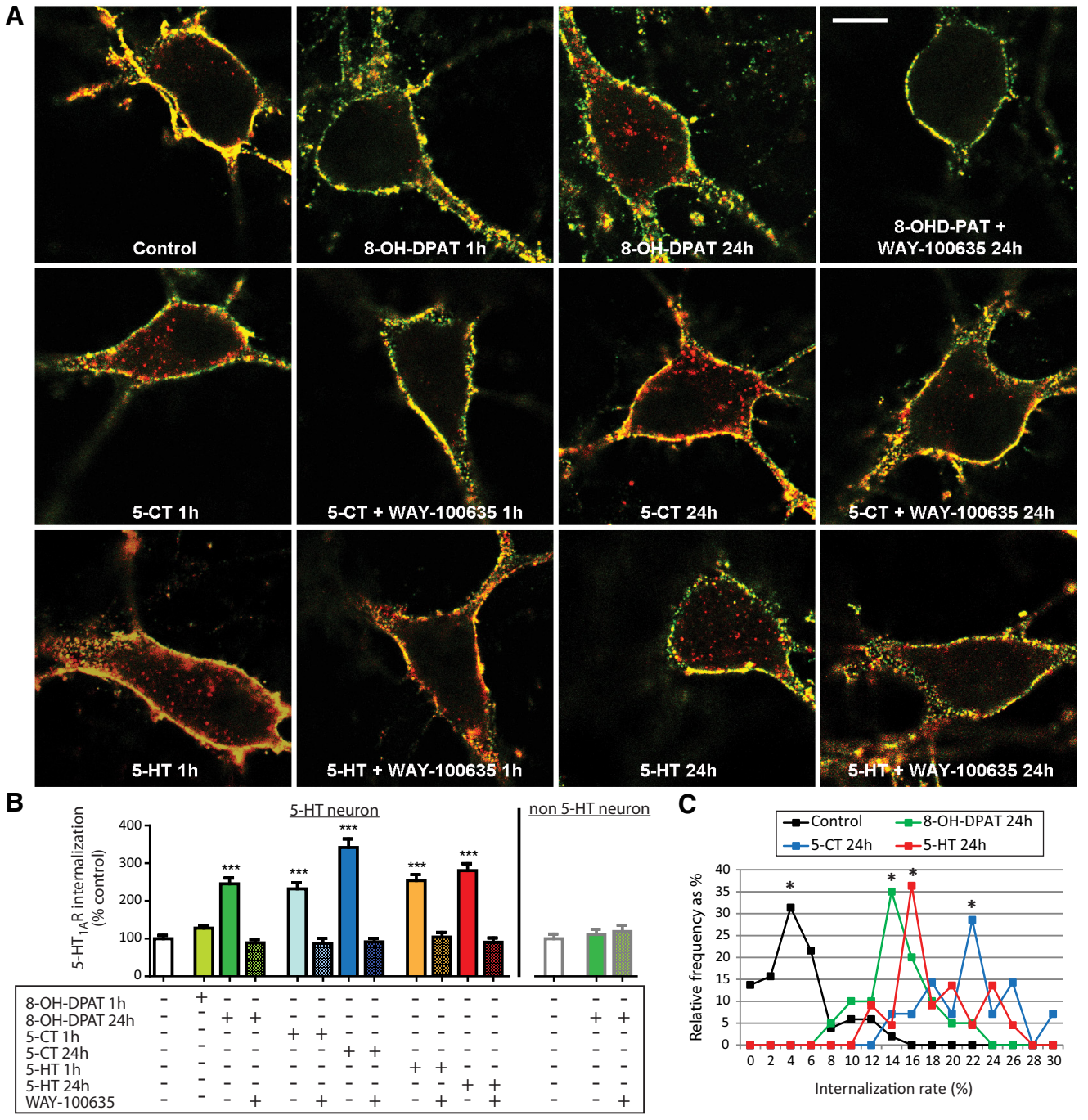

Figure 5. Effect of various pharmacological treatments on BBS-Flag-5-HT$_{1A}$R endocytosis in transduced neurons from raphe culture at 12–14 DIV. ***A***, Representative confocal microscopy fluorescence images of BBS-Flag-5-HT$_{1A}$R expressed in serotonergic raphe neurons in control conditions and after acute (1 h) or sustained (24 h) exposure to 5HT$_{1A}$R partial (8-OH-DPAT; 10 μM) or full agonists (5-CT, 1 μM; 5-HT, 10 μM) alone or in combination with antagonist (WAY-100635; 10 μM). BBS-Flag-5-HT$_{1A}$Rs localized at the plasma membrane were labeled in yellow (red and green colocalization), whereas internalized BBS-Flag-5-HT$_{1A}$Rs were identified by red labeling. Scale bar, 5 μm. ***B***, Quantification of internalized BBS-Flag-5-HT$_{1A}$R in raphe [serotonergic (5-HT) or non-5-HT] neurons in control conditions and after exposure to drugs. Bars indicate the mean ± SEM independent determinations in $n = 21$–55 individual cells. ***$p < 0.001$ as compared with control (Kruskal–Wallis test, Dunnett's test). ***C***, Frequency distribution (as percentage of total number of cells) of neurons displaying internalization rate in control condition or after sustained treatment with agonists (as percentage of control) with a bin width of 2% from 0 to 30% of internalization rate. Stars correspond to internalization peaks in control and pharmacological conditions.

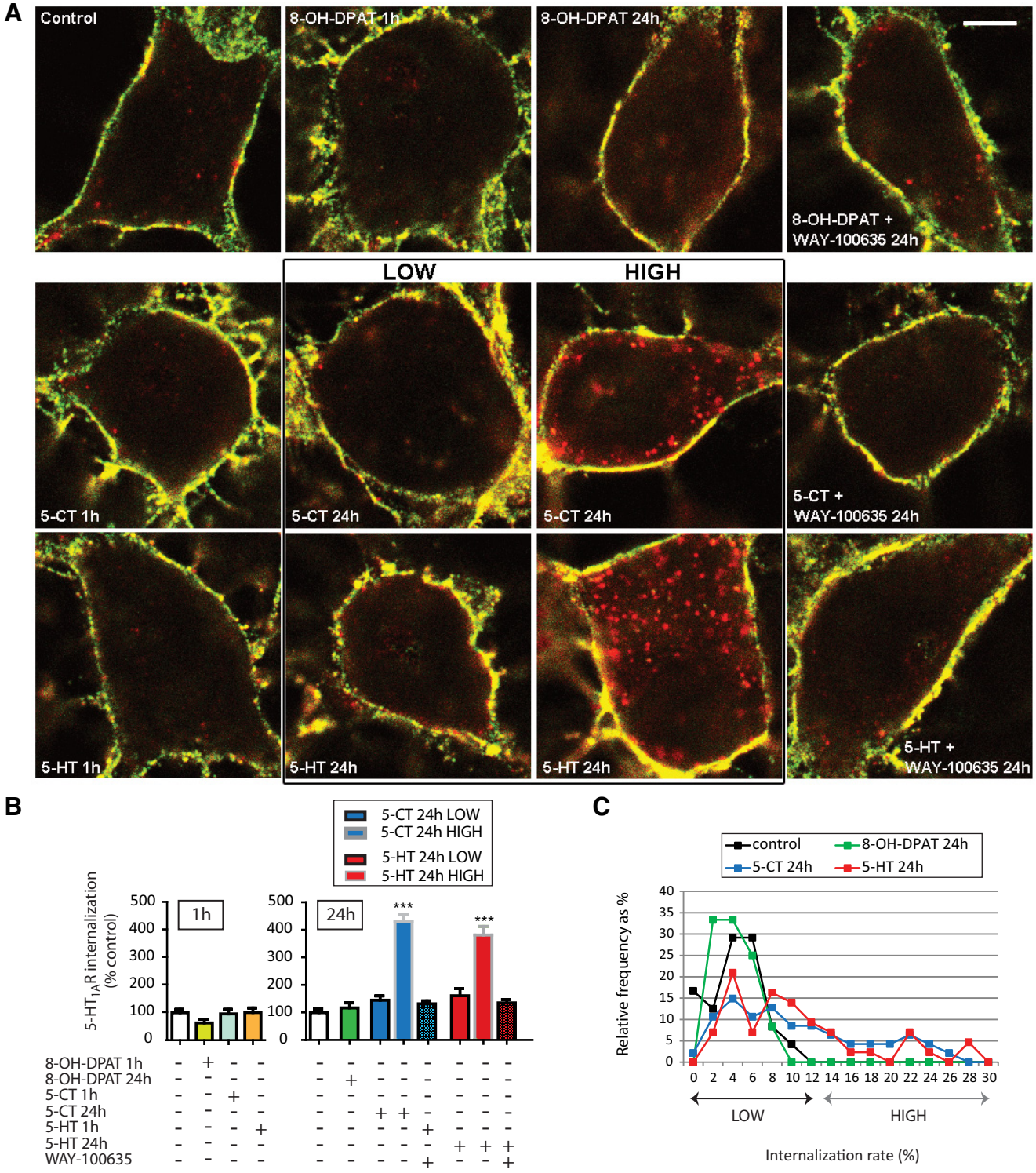

Figure 6. Effect of various pharmacological treatments on BBS-Flag-5-HT$_{1A}$R endocytosis in transduced hippocampal neurons at 12–14 DIV. ***A***, Representative confocal microscopy fluorescence images of BBS-Flag-5-HT$_{1A}$R expressed in hippocampal neurons in control conditions and after acute (1 h) or sustained (24 h) exposure to 5HT$_{1A}$R partial (8-OH-DPAT; 10 μM) or full agonists (5-CT, 1 μM; 5-HT, 10 μM) alone or in combination with antagonist (WAY-100635; 10 μM). For sustained treatments with 5-CT and 5-HT, populations of neurons could be divided into two classes depending on whether they presented agonist-induced internalization (high) or not (low). BBS-Flag-5-HT$_{1A}$Rs localized at the plasma membrane were labeled in yellow (red and green colocalization), whereas internalized BBS-Flag-5-HT$_{1A}$Rs were identified by red labeling. Scale bar, 5 μm. ***B***, Quantification of internalized BBS-Flag-5-HT$_{1A}$R in hippocampal neurons in control conditions and after acute or sustained exposure to drugs. For 5-CT and 5-HT sustained treatment, the two classes of neurons (low and high) were analyzed independently. Bars indicate the mean ± SEM independent determinations in $n = 21–55$ individual cells. ***$p < 0.001$ as compared with control (Kruskal–Wallis test, Dunnett's test). ***C***, Frequency distribution (as percentage of total number of cells) of neurons displaying internalization rate (as percentage of control) in control condition or after sustained treatment with agonists with a bin width of 2% from 0 to 30% of internalization rate.

Constitutive internalization of the 5-HT$_{1A}$R

Under basal conditions, without serum (i.e., without 5-HT) and any receptor ligand, internalization of tagged 5-HT$_{1A}$R was evidenced in both LLC-PK1 cells and neurons from hippocampus or raphe that expressed similar levels of the tagged receptor (Figs. 2, 4). BBS-tagged-5-HT$_{1A}$R internalization remained unchanged in raphe neurons exposed to WAY-100635 (10 μM), to prevent 5-HT$_{1A}$R stimulation by endogenous 5-HT produced by these neurons (but undetectable by HPLC-ED method), as expected of a constitutive process (Fig. 4). In LLC-PK1 cells, the tagged 5-HT$_{1A}$R followed a clathrin-dependent internalization pathway via a monensin-sensitive mechanism that involved fast recycling vesicles expressing the rab4 protein. Recycling of tagged 5-HT$_{1A}$R was evidenced in live microscopy experiments not only in LLC-PK1 cells (Fig. 3), but also in neurons (Fig. 4). In both models, receptor endocytosis was unrelated to the expression level of BBS-tagged-5-HT$_{1A}$R, suggesting that this process was not a consequence of some overexpression of the constructs. Accordingly, as already observed for other G-protein-coupled receptors (GPCRs), endocytosis might be essential to maintain homeostasis in 5-HT$_{1A}$R function and efficacy for serotonergic neurotransmission (Xu et al., 2007).

The existence of a possible relationship between constitutive activity and constitutive endocytosis of the 5-HT$_{1A}$R could be excluded in LLC-PK1 cells because inverse agonists such as methiothepin and spiperone (Martel et al., 2007) did not affect BBS-5-HT$_{1A}$R constitutive internalization. This conclusion very probably applied also to neurons because only a nonsignificant tendency to a decrease in BBS-5-HT$_{1A}$R internalization was observed in raphe neurons exposed to spiperone (Fig. 4).

The function of 5-HT$_{1A}$R constitutive endocytosis and recycling, in particular in soma and dendrites of neurons, could be different from that typically identified for other GPCRs, such as receptor targeting to axons or regulation of efficacy of synaptic transmission that are commonly reversed by stimulation of the receptor by inverse agonists (Pula et al., 2004; Carrel et al., 2011). Recently, it has been proposed that constitutive endocytosis and recycling to the plasma membrane of dopamine D_2 receptor in cultured mouse striatal medium spiny neurons (following similar pathway to the one observed for BBS-5-HT$_{1A}$R) has a function in maintaining steady-state levels of functional D_2 receptors (Li et al., 2012). In neurons, after internalization, vesicles endowed with tagged 5-HT$_{1A}$R were trafficking into the soma to be targeted back to the cell membrane or transported inside the neurons from the soma into dendrites (Fig. 4). We can postulate that 5-HT$_{1A}$R constitutive endocytosis/recycling events are involved in "re-targeting" of receptors to specific postsynaptic sites so as to modulate receptor function. For glutamate or GABA ionotropic receptors, intracellular trafficking and rapid lateral diffusion within the synaptic area have been shown to play a key role for regulating the density of these receptors in the postsynaptic membrane (Bard et al., 2011). Previous studies also showed that dopamine D_1 receptors move by lateral diffusion in the plasma membrane of striatal neurons and that activation of NMDA receptors slows down this process via *trans*-regulatory mechanisms (Scott et al., 2006). Whether constitutive endocytosis/recycling of 5-HT$_{1A}$R could also depend on activation of other receptor types for regulating their homeostatic state and function is also a relevant question to be addressed in future studies.

Agonist-induced internalization of the 5-HT$_{1A}$R

Our study demonstrated that no agonist-promoted BBS-5-HT$_{1A}$R endocytosis was found in transfected LLC-PK1 cells, and this could not be attributed to an inhibitory effect of BTX binding on the ability of agonists to activate the receptor, because BTX did not interfere with receptor responses to various 5-HT$_{1A}$R ligands (Fig. 1). This absence of agonist-induced endocytosis has been reported for the 5-HT$_{1A}$R in several studies on different cell lines (Pucadyil et al., 2004; Renner et al., 2012), whereas an effect was reported in other studies (Della Rocca et al., 1999; Heusler et al., 2008). Such differences suggest that agonist-induced 5-HT$_{1A}$R internalization depends strongly on the recombinant vectors used for 5-HT$_{1A}$R expression, the cell type, and very probably other experimental conditions. Studies of 5-HT$_{1A}$R trafficking in the LLC-PK1 cell line clearly provided relevant data on the existence of constitutive internalization and its underlying mechanisms, but this cellular model has limitations, because the cellular machinery is different in epithelial cells and in neurons. Therefore, we also studied 5-HT$_{1A}$R distribution and trafficking in cultured neurons exposed to agonists. Although transfected neurons overexpressed BBS-5-HT$_{1A}$R, care was taken to compare neurons from raphe and hippocampus that expressed similar levels of receptors. Moreover, we verified that pharmacological treatments did not modify the expression rate of receptors (Table 1). Under these conditions, 5-HT$_{1A}$R stimulation by full agonists (5-HT and 5-CT; Assié et al., 1999) for 1 h induced BBS-5-HT$_{1A}$R internalization in serotonergic raphe but not in hippocampal neurons (Figs. 5, 6). Such a difference meets the *in vivo* data reported by Riad et al. (2001) who showed that acute treatment with the SSRI fluoxetine induced 5-HT$_{1A}$R internalization (visualized by electron microscopy with specific antibodies) in dorsal raphe nucleus but not hippocampus in rats. In our studies, we were able to visualize a different level of internalization depending on the efficacy of agonists. Although the three agonists tested triggered BBS-5-HT$_{1A}$R internalization in serotonergic raphe neurons after a 24 h exposure to these ligands (Fig. 5), the full agonists 5-CT and 5-HT, but not the partial agonist 8-OH-DPAT, were able to induce this process after an exposure of only 1 h. In contrast, in hippocampal neurons, no internalization was observed even after a 24 h exposure to the partial agonist 8-OH-DPAT. Furthermore, after such a sustained treatment, the full agonists were able to induce receptor endocytosis (up to 400%) in only a subpopulation of hippocampal (HIGH) neurons, thereby reflecting the existence of a heterogeneous population of neurons in hippocampal cultures. Whereas 5-HT$_{1A}$R is expressed almost exclusively in serotonergic neurons in the raphe area in rats (Yasufuku-Takano et al., 2008; Kiyasova et al., 2013), only pyramidal neurons (mainly in CA1 subarea) are expressing endogenously 5-HT$_{1A}$R in the hippocampus (Riad et al., 2001). Differences between hippocampal neurons that exhibit (HIGH) or not (LOW) 5-HT- or 5-CT-induced BBS-5-HT$_{1A}$R internalization probably relied on their respective phenotypic characteristics (endogenous expression of the 5-HT$_{1A}$R, different coupling pathways, or expression of specific proteins) that remain to be identified.

The data obtained with serotonergic neurons suggest that regulation of 5-HT$_{1A}$ autoreceptor internalization presumably involves intracellular modulation of the machinery necessary for endocytosis, and the sustained stimulation of the receptor per se could be responsible for this modulation. Indeed, modulation of dynamin expression and localization was shown to be responsible for the increased ability of μ-opioid receptors to internalize in enteric neurons after chronic treatment (Patierno at al., 2011). Moreover, the lack of internalization in the majority of hippocampal neurons exposed to agonists is in line with previous results that demonstrated that no adaptive changes (desensitiza-

tion) occurred in hippocampus after acute or chronic stimulation, either by exogenous 5-HT$_{1A}$R agonist or by 5-HT under SSRI treatment (Lanfumey and Hamon, 2000; Le Poul et al., 2000; Hensler, 2003). 5-HT$_{1A}$R are G$_{i/o}$-coupled receptors but the type of inhibitory α-subunit differs in raphe (preferentially Gαi3) and in brain areas receiving serotonergic projections such as the hippocampus (preferentially Gαo) (Mannoury La Cour et al., 2006). These differences could contribute to differences in signaling pathways, and possibly in traffic regulation after receptor stimulation. In particular, 5-HT$_{1A}$R stimulation was found to decrease ERK phosphorylation in the hippocampus (Chen et al., 2002) but to rapidly increase this process in the raphe (Sullivan et al., 2005). As MAPK pathways regulate gene expression and physiological response, such differential changes could account for long-term neuronal adaptations after chronic SSRI treatment in the raphe but not in the hippocampus.

Antidepressant efficacy of SSRI requires 3–4 weeks of treatment with these drugs, a delay which corresponds to the time necessary for 5-HT$_{1A}$ autoreceptor desensitization (Artigas et al., 1994; Lanfumey and Hamon, 2000; Blier and Ward, 2003). Clinical trials explored the possibility to decrease SSRI delay of action by blocking 5-HT$_{1A}$ receptors (Artigas et al., 1994; Geretsegger et al., 2008). However, whereas blocking 5-HT$_{1A}$ autoreceptor activation could have a beneficial effect by inhibiting 5-HT$_{1A}$ autoreceptor-mediated feedback on serotonin release, adverse effects could occur on the therapeutic action of antidepressant drugs due to the beneficial effect of stimulating postsynaptic 5-HT$_{1A}$R in corticolimbic areas (Celada et al., 2013). Combining 5-HT$_{1A}$R partial agonism with SERT inhibition by administering SSRI and pindolol (acting as a partial 5-HT$_{1A}$R agonist) or new antidepressant drugs such as vilazodone and vortioxetine (with pharmacological profiles that combine SSRI and partial 5-HT$_{1A}$R agonist properties) appeared to be more efficient (Hamon and Blier, 2013). These pharmacological strategies presumably achieve beneficial effects on depression treatment by increasing extracellular 5-HT and promoting 5-HT$_{1A}$ autoreceptor internalization to limit the inhibitory feedback loop on 5-HT release (Stahl et al., 2013).

References

Albert PR, Zhou QY, Van Tol HH, Bunzow JR, Civelli O (1990) Cloning, functional expression, and mRNA tissue distribution of the rat 5-hydroxytryptamine1A receptor gene. J Biol Chem 265:5825–5832. Medline

Artigas F, Perez V, Alvarez E (1994) Pindolol induces a rapid improvement of depressed patients treated with serotonin reuptake inhibitors. Arch Gen Psychiatry 51:248–251. CrossRef Medline

Assié MB, Cosi C, Koek W (1999) Correlation between low/high affinity ratios for 5-HT$_{1A}$ receptors and intrinsic activity. Eur J Pharmacol 386: 97–103. CrossRef Medline

Bard L, Groc L (2011) Glutamate receptor dynamics and protein interaction: lessons from the NMDA receptor. Mol Cell Neurosci 48:298–307. CrossRef Medline

Blier P, Ward NM (2003) Is there a role for 5-HT$_{1A}$ agonists in the treatment of depression? Biol Psychiatry 53:193–203. CrossRef Medline

Carrel D, Hamon M, Darmon M (2006) Role of the C-terminal di-leucine motif of 5-HT1A and 5-HT1B serotonin receptors in plasma membrane targeting. J Cell Sci 119:4276–4284. CrossRef Medline

Carrel D, Simon A, Emerit MB, Rivals I, Leterrier C, Biard M, Hamon M, Darmon M, Lenkei Z (2011) Axonal targeting of the 5-HT1B serotonin receptor relies on structure-specific constitutive activation. Traffic 12: 1501–1520. CrossRef Medline

Celada P, Bortolozzi A, Artigas F (2013) Serotonin 5-HT1A receptors as targets for agents to treat psychiatric disorders: rationale and current status of research. CNS Drugs 27:703–716. CrossRef Medline

Chen J, Shen C, Meller E (2002) 5-HT1A receptor-mediated regulation of mitogen-activated protein kinase phosphorylation in rat brain. Eur J Pharmacol 452:155–162. CrossRef Medline

Cowen DS, Molinoff PB, Manning DR (1997) 5-hydroxytryptamine1A receptor-mediated increases in receptor expression and activation of nuclear factor-kappaB in transfected Chinese hamster ovary cells. Mol Pharmacol 52:221–226. Medline

Darmon M, Langlois X, Suffisseau L, Fattaccini CM, Hamon M (1998) Differential membrane targeting and pharmacological characterization of chimeras of rat serotonin 5-HT1A and 5-HT1B receptors expressed in epithelial LLC-PK1 cells. J Neurochem 71:2294–2303. Medline

Della Rocca GJ, Mukhin YV, Garnovskaya MN, Daaka Y, Clark GJ, Luttrell LM, Lefkowitz RJ, Raymond JR (1999) Serotonin 5-HT1A receptor-mediated Erk activation requires calcium/calmodulin-dependent receptor endocytosis. J Biol Chem 274:4749–4753. CrossRef Medline

Geretsegger C, Bitterlich W, Stelzig R, Stuppaeck C, Bondy B, Aichhorn W (2008) Paroxetine with pindolol augmentation: a double-blind, randomized, placebo-controlled study in depressed in-patients. Eur Neuropsychopharmacol 18:141–146. CrossRef Medline

Hamon M, Blier P (2013) Monoamine neurocircuitry in depression and strategies for new treatments. Prog Neuropsychopharmacol Biol Psychiatry 45:54–63. CrossRef Medline

Hannan S, Wilkins ME, Dehghani-Tafti E, Thomas P, Baddeley SM, Smart TG (2011) Gamma-aminobutyric acid type B (GABA(B)) receptor internalization is regulated by the R2 subunit. J Biol Chem 286:24324–24335. CrossRef Medline

Hensler JG (2003) Regulation of 5-HT1A receptor function in brain following agonist or antidepressant administration. Life Sci 72:1665–1682. CrossRef Medline

Heusler P, Newman-Tancredi A, Loock T, Cussac D (2008) Antipsychotics differ in their ability to internalise human dopamine D2S and human serotonin 5-HT1A receptors in HEK293 cells. Eur J Pharmacol 581:37–46. CrossRef Medline

Jolimay N, Franck L, Langlois X, Hamon M, Darmon M (2000) Dominant role of the cytosolic C-terminal domain of the rat 5-HT1B receptor in axonal-apical targeting. J Neurosci 20:9111–9118. Medline

Kiyasova V, Bonnavion P, Scotto-Lomassese S, Fabre V, Sahly I, Tronche F, Deneris E, Gaspar P, Fernandez SP (2013) A subpopulation of serotonergic neurons that do not express the 5-HT1A autoreceptor. ACS Chem Neurosci 4:89–95. CrossRef Medline

Lanfumey L, Hamon M (2000) Central 5-HT(1A) receptors: regional distribution and functional characteristics. Nucl Med Biol 27:429–435. CrossRef Medline

Langlois X, el Mestikawy S, Arpin M, Triller A, Hamon M, Darmon M (1996) Differential addressing of 5-HT1A and 5-HT1B receptors in transfected LLC-PK1 epithelial cells: a model of receptor targeting in neurons. Neuroscience 74:297–302. CrossRef Medline

Le Poul E, Boni C, Hanoun N, Laporte AM, Laaris N, Chauveau J, Hamon M, Lanfumey L (2000) Differential adaptation of brain 5-HT1A and 5-HT1B receptors and 5-HT transporter in rats treated chronically with fluoxetine. Neuropharmacology 39:110–122. CrossRef Medline

Li Y, Roy BD, Wang W, Zhang L, Sampson SB, Yang Y, Lin DT (2012) Identification of two functionally distinct endosomal recycling pathways for dopamine D(2) receptor. J Neurosci 32:7178–7190. CrossRef Medline

Mannoury la Cour C, El Mestikawy S, Hanoun N, Hamon M, Lanfumey L (2006) Regional differences in the coupling of 5-hydroxytryptamine-1A receptors to G proteins in the rat brain. Mol Pharmacol 70:1013–1021. CrossRef Medline

Martel JC, Ormière AM, Leduc N, Assié MB, Cussac D, Newman-Tancredi A (2007) Native rat hippocampal 5-HT$_{1A}$ receptors show constitutive activity. Mol Pharmacol 71:638–643. Medline

Morton RA, Luo G, Davis MI, Hales TG, Lovinger DM (2011) Fluorophore assisted light inactivation (FALI) of recombinant 5-HTA receptor constitutive internalization and function. Mol Cell Neurosci 47:79–92. CrossRef Medline

Patierno S, Anselmi L, Jaramillo I, Scott D, Garcia R, Sternini C (2011) Morphine induces μ opioid receptor endocytosis in guinea pig enteric neurons following prolonged receptor activation. Gastroenterology 140: 618–626. CrossRef Medline

Poulain FE, Chauvin S, Wehrlé R, Desclaux M, Mallet J, Vodjdani G, Dusart I, Sobel A (2008) SCLIP is crucial for the formation and development of the Purkinje cell dendritic arbor. J Neurosci 28:7387–7398. CrossRef Medline

Pucadyil TJ, Kalipatnapu S, Harikumar KG, Rangaraj N, Karnik SS, Chattopadhyay A (2004) G-protein-dependent cell surface dynamics of the human serotonin1A receptor tagged to yellow fluorescent protein. Biochemistry 43:15852–15862. CrossRef Medline

Pula G, Mundell SJ, Roberts PJ, Kelly E (2004) Agonist-independent internalization of metabotropic glutamate receptor 1a is arrestin- and clathrin-dependent and is suppressed by receptor inverse agonists. J Neurochem 89:1009–1020. CrossRef Medline

Renner U, Zeug A, Woehler A, Niebert M, Dityatev A, Dityateva G, Gorinski N, Guseva D, Abdel-Galil D, Frohlich M, Doring F, Wischmeyer E, Richter DW, Neher E, Ponimaskin EG (2012) Heterodimerization of serotonin receptors 5-HT1A and 5-HT7 differentially regulates receptor signalling and trafficking. J Cell Sci 2486–2499.

Riad M, Watkins KC, Doucet E, Hamon M, Descarries L (2001) Agonist-induced internalization of serotonin-1a receptors in the dorsal raphe nucleus (autoreceptors) but not hippocampus (heteroreceptors). J Neurosci 21:8378–8386. Medline

Riad M, Zimmer L, Rbah L, Watkins KC, Hamon M, Descarries L (2004) Acute treatment with the antidepressant fluoxetine internalizes 5-HT1A autoreceptors and reduces the in vivo binding of the PET radioligand [18F]MPPF in the nucleus raphe dorsalis of rat. J Neurosci 24:5420–5426. CrossRef Medline

Riad M, Rbah L, Verdurand M, Aznavour N, Zimmer L, Descarries L (2008) Unchanged density of 5-HT(1A) autoreceptors on the plasma membrane of nucleus raphe dorsalis neurons in rats chronically treated with fluoxetine. Neuroscience 151:692–700. CrossRef Medline

Rosenfeld JL, Knoll BJ, Moore RH (2002) Regulation of G-protein-coupled receptor activity by rab GTPases. Receptors Channels 8:87–97. CrossRef Medline

Scott L, Zelenin S, Malmersjö S, Kowalewski JM, Markus EZ, Nairn AC, Greengard P, Brismar H, Aperia A (2006) Allosteric changes of the NMDA receptor trap diffusible dopamine 1 receptors in spines. Proc Natl Acad Sci U S A 103:762–767. CrossRef Medline

Seachrist JL, Ferguson SS (2003) Regulation of G protein-coupled receptor endocytosis and trafficking by Rab GTPases. Life Sci 74:225–235. CrossRef Medline

Sekine-Aizawa Y, Huganir RL (2004) Imaging of receptor trafficking by using alpha-bungarotoxin-binding-site-tagged receptors. Proc Natl Acad Sci U S A 101:17114–17119. CrossRef Medline

Sönnichsen B, De Renzis S, Nielsen E, Rietdorf J, Zerial M (2000) Distinct membrane domains on endosomes in the recycling pathway visualized by multicolor imaging of Rab4, Rab5, and Rab11. J Cell Biol 149:901–914. CrossRef Medline

Stahl SM, Lee-Zimmerman C, Cartwright S, Morrissette DA (2013) Serotonergic drugs for depression and beyond. Curr Drug Targets 14:578–585. CrossRef Medline

Stein BS, Bensch KG, Sussman HH (1984) Complete inhibition of transferrin recycling by monensin in K562 cells. J Biol Chem 259:14762–14772. Medline

Sullivan NR, Crane JW, Damjanoska KJ, Carrasco GA, D'Souza DN, Garcia F, Van de Kar LD (2005) Tandospirone activates neuroendocrine and ERK (MAP kinase) signaling pathways specifically through 5-HT1A receptor mechanisms in vivo. Naunyn Schmiedebergs Arch Pharmacol 371:18–26. CrossRef Medline

Xu ZQ, Zhang X, Scott L (2007) Regulation of G protein-coupled receptor trafficking. Acta Physiol 190:39–45. CrossRef Medline

Yasufuku-Takano J, Nakajima S, Nakajima Y (2008) Morphological and physiological properties of serotonergic neurons in dissociated cultures from the postnatal rat dorsal raphe nucleus. J Neurosci Methods 167:258–267. CrossRef Medline

Zennou V, Petit C, Guetard D, Nerhbass U, Montagnier L, Charneau P (2000) HIV-1 genome nuclear import is mediated by a central DNA flap. Cell 101:173–185. CrossRef Medline